Non-contact Voltage Measurement Technique for On-Line Monitoring of Transient Overvoltages

G. D. P. Mahidhar, Patrick Janus, Hans Edin
School of Electrical Engineering and Computer Science, KTH – Royal Institute of Technology, Stockholm, Sweden, SE-10044
gorla@kth.se

Abstract

The electric power system is continuously growing in its size, complexity and required reliability. There is an increased risk due to transient overvoltages which can deteriorate the insulation for different power system components. There is a need for monitoring of transient voltages to better monitor the effects due to them on the insulation of the components. It can be achieved using a non-contact voltage measurement technique. The study elucidates the theory and practical application of the non-contact voltage measurements. The measurement of voltage is achieved by utilizing the stray parasitic capacitance between the high voltage conductor and the ground. A metal plate is used as a sensor to detect the voltage, which indirectly acts as a capacitance divider for voltage measurement. The current study uses operational amplifier based differential-integrator circuit topology in order to accurately measure the voltage over a wide bandwidth of 20 Hz - 1 MHz. The measurement technique is used for measurement of three phase voltages and a methodology is proposed for it. The sensor system is also tested in an online test scenario in a substation for monitoring the shunt reactor switching transients.

1. Introduction

With the growing power demand, the power system network is also growing faster in its size, complexity and reliability requirements. In the large power systems, with the integration of newer technologies like wind and solar power, there is also an increased risk related to power loss and unstable power supply conditions leading to reduced reliability. Such unavoidable situations can give rise to transient overvoltages which can be dangerous for the insulation of power system components. These transients can be caused due to lightning strikes or due to switching transients caused by switching in and out equipment [1, 2]. Therefore, it has always been an interest for the researchers to develop methods for detection and mitigation of the effects caused by the transient overvoltages. Over the years, many different techniques for transient overvoltage monitoring were introduced. Some of the standard techniques are using capacitance dividers, capacitive voltage transformers, MOV dividers, RC dividers, etc. [3]. But all the techniques need a contact point in the power circuit in order to measure and requires additional equipment and space.

From the past few decades, researchers have investigated on non-contact voltage measurement techniques based on electric field measurements [4, 5]. Another such technique is with the usage of metal plate as a capacitive sensor that uses the stray capacitance between the high voltage conductor and metal plate and the metal plate and ground as the arms of a capacitance voltage divider. Such systems utilized the concept of differentiation-integration (D-I) method using the passive components in order to measure the voltages [6, 7]. In the recent years, using the active analog electronic integrated circuits, researchers were able to implement the D-I topology with improved sensitivity and lower noise [8, 9]. There are few studies conducted on models of the three phase conductors and the non-contact voltage measurements were tested [10]. Studies were also conducted in the on-site measurements for three phase voltages in order to monitor the overvoltages [11, 12].

The current study focuses on the aspects related to the principle and measurement of three phase voltages in a non-contact method using the metal plate sensor. The measurements were well tested in a laboratory model. The test method was tested in a 220 kV substation for measuring switching in connection to switching in and out a shunt reactor.

2. Working Principle

The important concept for non-contact voltage measurement is capacitive sensing. A metal plate placed on safe distance from the high voltage, and therefore near "ground" is used in order to detect the voltages on the high voltage conductors. By placing the sensor near to the ground, the danger due to high voltages can be eliminated and the contact from the electrical network can be avoided. By utilising the stray capacitance between the conductor and the metal plate, there are small capacitive currents flowing due to electrostatic induction. The currents sensed are proportional to the time differential of the potential on the HV conductors. An integrator can be used to acquire signal that is proportional to the actual voltage. Figure 1 shows the schematic for the measurement based on the D-I principle. To obtain the function of integration, an operational amplifier (OP AMP) based integrator circuit

is implemented. An LMC 6001 ultra-low input current OP- AMP which is suitable for the present case was used in two stages. First the signal is integrated by integrator stage and amplified by gain stage to improve the signal to noise ratio [13]. Figure 2 shows the details related to the circuit schematic used for measurements. By analysing the circuit, the current drawn by the parasitic elements i.e. by C_{HV} and C_E is given by i_c. The C_E is very high compared to C_{HV} as the metal plate is very close to ground making Z_{HV} much higher than Z_E. With this assumption, the contribution due to C_E is neglected in the circuit analysis. At this stage, the current induced on the metal plate is directly proportional to the differential of the voltage (v_{in}).

$$i_c = \frac{v_{in}}{z_{HV}+z_E} \approx \frac{v_{in}}{z_{HV}} = sC_{HV}v_{in} \quad (1)$$

The next step of integration is carried out using the OP AMP circuit. The overall transfer function of the OP AMP circuit is given by H_c in equation 2. Figure 3(a) and 3(b) gives the theoretical bode plot for the H_c showing the magnitude and phase plots for the circuit. Equation 3 also gives the H_c but from the perspective of D-I circuit response. By expanding i_c and rearranging equation 3, the transfer function for the overall circuit response is obtained. The calibration factor, K_f is dependent only on the circuit parameters and can be calculated. C_{HV} is dependent on the test geometry. The calculated K_f for the current study is calculated to $0.232 \times 10^9\ \Omega/s$.

$$H_c(s) = \frac{sR_fC_1}{(sR_fC_f+1)(sR_1C_1+1)} \times \frac{R_a+R_b}{R_a} \quad (2)$$

$$H_c(s) = \frac{v_{out}(s)}{i_c(s)} = \frac{v_{out}(s)}{sC_{HV}v_{in}(s)} \quad (3)$$

$$\frac{v_{out}(s)}{v_{in}(s)} = sC_{HV}H_c(s) = K_fC_{HV} \quad (4)$$

$$K_f = sH_c(s) \quad (5)$$

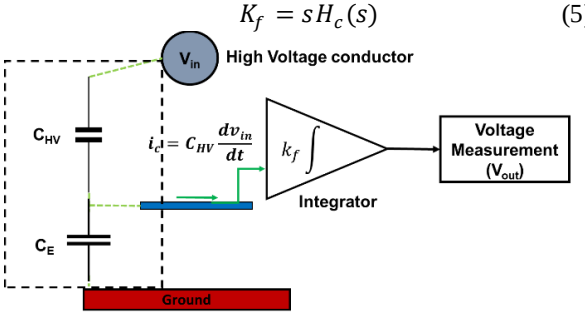

Fig. 1. Working principle of non-contact voltage measurement by Differentiation Integration method

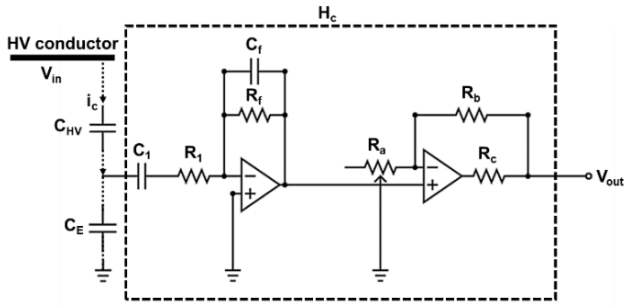

Fig. 2. Schematic of the circuit for measurement

3. Experimental Setup

Based on the theoretical concepts related to the non-contact voltage measurement, a laboratory test model was arranged to emulate the condition present at a three phase transmission line. Three cylindrical hollow copper rods were suspended and were used as high voltage conductors connected to a three-phase high voltage transformer. Steel sheets were placed on the ground and earthed. Three sensors of rectangular plate (10 cm × 40 cm) made of aluminium were used as sensors to measure the voltage on the conductor. Figure 4(a) and 4(b) shows the geometric dimensions of the model and a photo of the lab model with sensors respectively. Three Tektronix high voltage probes P6015 were used for measuring the voltage at the transformer high voltage terminals. Two Four-channel Keysight DSOX2014A 200 MHz oscilloscopes were used for measuring the probe and sensor voltages at 1 MSa/s.

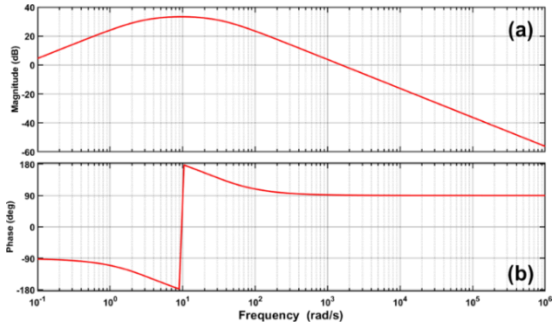

Fig. 3. (a) Magnitude response, (b) Phase response of the of the OP AMP integrator circuit

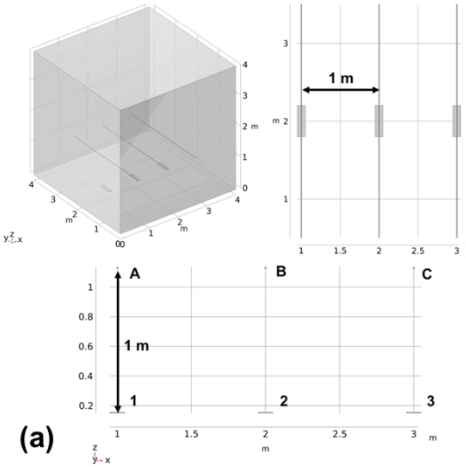

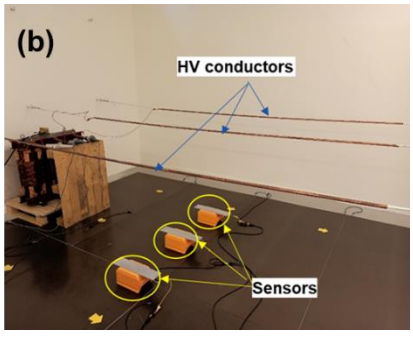

Fig. 4. Geometry of the test room and the setup

4. Experimental Results and Discussion

To test the performance of the sensor system, a 5 kVpp 50 Hz AC voltage was applied on the conductors and the measurement is carried out. Figure 5 shows the voltages on three phases measured using the HV probes and Figure 6 shows the voltages measured using the sensor system. From the results, it is clear that there is mismatch in phases and amplitudes of the sensor measurements. This mismatch is caused because of the cross-capacitive couplings between a sensor and the two high voltage conductors that are not above it. In order to measure the actual voltage on a particular conductor, the sensor measurements need to be decoupled from the voltages that are capacitively influenced from the other conductors. Hence, a decoupling strategy is needed in order to estimate the actual voltages on the conductors. Figure 7 shows a representative figure of all the capacitances that can influence the measurement technique. In the current work, the voltages on the conductors are considered as 3- phase symmetrical voltages. In this case, the voltages induced by the conductors on other conductors is nullified because of symmetric three-phase voltage supply. Similar analogy can be used for the case of capacitances between sensors. Because of this feature, the mutual capacitances between the phase conductors, conductor-ground and sensor-ground are neglected in the model as the contribution due to them is very small. From Figure 7, the capacitances that are represented by green dashed lines contribute majorly to the voltages on the sensors. Voltages on the conductors are v_a, v_b, v_c. The currents induced on the sensors are i_1, i_2, i_3. Voltages sensed by the sensors are v_{s1}, v_{s2}, v_{s3}. The sensed voltage by the sensor is dependent on the voltage on all the three conductors and the capacitance associated between them. This condition can be formulated as a set of linear equations to solve for three unknown voltages using the three known voltages. Based on the theory, the following set of equations related to the currents induced on the sensors are formulated in order to solve for the actual voltages on the phase conductors.

$$i_1 = C_{a1}\frac{dv_a}{dt} + C_{a2}\frac{dv_b}{dt} + C_{a3}\frac{dv_c}{dt} \quad (6)$$

$$i_2 = C_{b1}\frac{dv_a}{dt} + C_{b2}\frac{dv_b}{dt} + C_{b3}\frac{dv_c}{dt} \quad (7)$$

$$i_3 = C_{c1}\frac{dv_a}{dt} + C_{c2}\frac{dv_b}{dt} + C_{c3}\frac{dv_c}{dt} \quad (8)$$

The induced currents on the sensors are integrated and amplified leading to the sensed voltages, given in equations 9, 10 and 11. These linear equations can be represented in matrix form as given in equation 12. K_f is the calibration factor of the integrator module which is a constant that can be multiplied to the capacitance matrix (C_{mat}) in order to get the sensor response matrix (G_{mat}). In order to solve for the actual voltages (V_{real}), the inverse of the G_{mat} is multiplied with sensor voltages.

$$v_{s1} = K_f(C_{a1}v_a + C_{a2}v_b + C_{a3}v_c) \quad (9)$$

$$v_{s2} = K_f(C_{b1}v_a + C_{b2}v_b + C_{b3}v_c) \quad (10)$$

$$v_{s3} = K_f(C_{c1}v_a + C_{c2}v_b + C_{c3}v_c) \quad (11)$$

$$\begin{bmatrix} v_{s1} \\ v_{s2} \\ v_{s3} \end{bmatrix} = K_f \times \begin{bmatrix} C_{a1} & C_{a2} & C_{a3} \\ C_{b1} & C_{b2} & C_{b3} \\ C_{c1} & C_{c2} & C_{c3} \end{bmatrix} \times \begin{bmatrix} v_a \\ v_b \\ v_c \end{bmatrix} \quad (12)$$

$$[V_s] = K_f \times [C_{mat}] \times [V_{real}] \quad (13)$$

$$[V_s] = [G_{mat}] \times [V_{real}] \quad (14)$$

$$[V_{real}] = [G_{mat}]^{-1} \times [V_s] \quad (15)$$

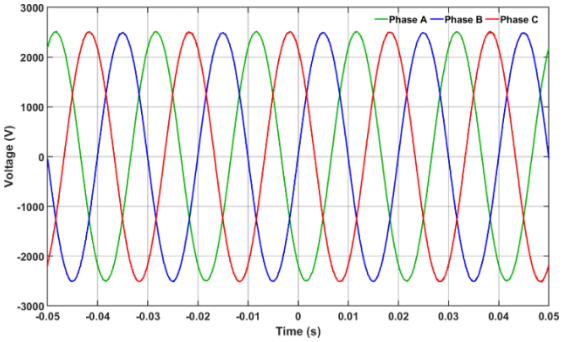

Fig. 5. Three phase voltages measured with the probe

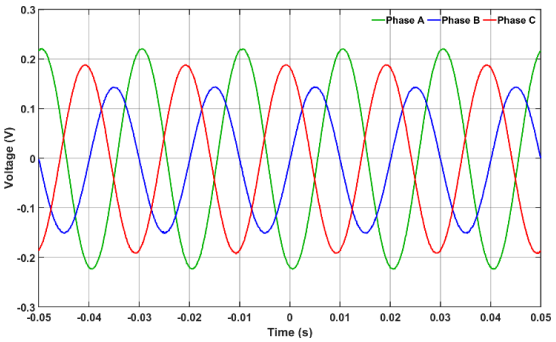

Fig. 6. Response of the sensors to three phase voltages

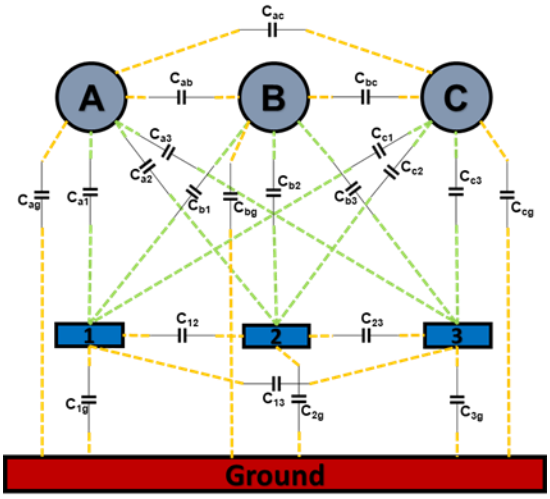

Fig. 7. Representation of capacitances in three phase transmission line system with sensors

The same procedure can be applied in the case of the laboratory model also in order to calculate the actual voltages. The capacitance matrix for the laboratory model can be estimated using the COMSOL

Multiphysics. A 3D stationary sweep study is carried out in order to calculate the complete capacitance matrix that gives the full information of capacitances between the conductors and sensors. A 3D study is carried out in order to obtain capacitances close to the real values. Using this method, the calculated capacitance matrix of the laboratory test model is given in equation 16.

$$C_{mat} = \begin{bmatrix} 0.4667 & 0.1705 & 0.0309 \\ 0.16177 & 0.4245 & 0.1607 \\ 0.0300 & 0.1607 & 0.4067 \end{bmatrix} pF \qquad (16)$$

Using the information of capacitance matrix and the sensed voltages, decoupling is carried out and the actual voltages on the conductors are reconstructed. These voltages are compared with the probe voltages and are shown in Figure 8. From the figure it can be clearly seen that the waveforms of reconstructed and the actual voltages are nearly matching, and the absolute error is less than 5% for all the waveforms.

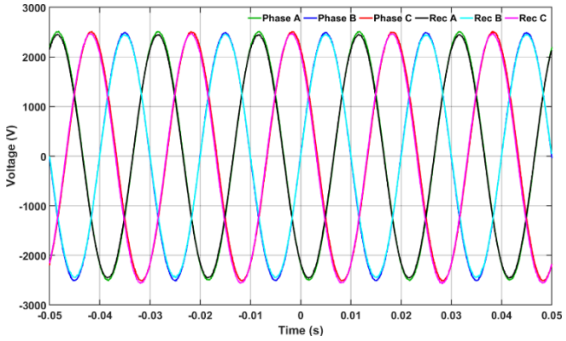

Fig. 8. Comparison of the actual voltages to the voltages reconstructed using the sensed voltages

To further test the measurement technique under transient voltage conditions, a short duration DC voltage was introduced in order to generate transient overvoltage condition. Figure 9 shows the comparison between the probe voltage and the sensor voltages during the transient condition and the measurements match well with the actual voltages.

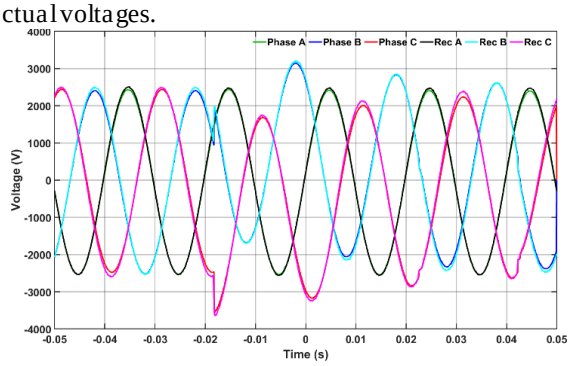

Fig. 9. Comparison of the actual voltages and sensed voltages during transient events

After successful laboratory testing of the measurement principle, the sensors and the measurement system were tested in a real case. The measurements were carried out at a 220 kV, 150 MVAr shunt reactor at Svenska Kraftnät's Hagby substation, Stockholm, Sweden. An online monitoring system was devised to monitor the switching transients of the shunt reactor. The capacitive sensors were placed in a bay that connects the shunt reactor under the three phase line.

Figure 10 shows the google maps image of the substation's part where the online sensor system is installed near a shunt reactor. The 3D geometric model of the shunt reactor bay and its surroundings are shown in Figure 11. It is used for the calculation of the capacitance matrix for decoupling of sensor voltages. The steel supports and the unused bay beside the reactor bay was also included in the model to improve the accuracy of the capacitance matrix calculation. The capacitance matrix calculated using COMSOL is given in equation 17.

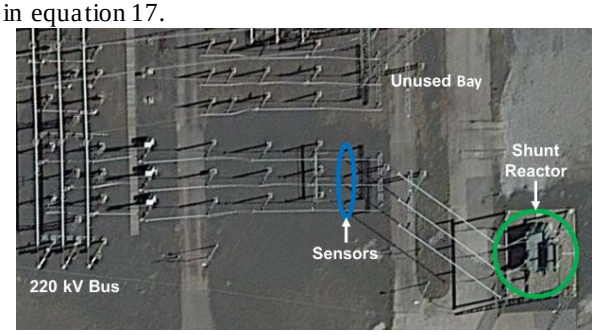

Fig. 10. Google Maps image of the part of substation with shunt reactor [13]

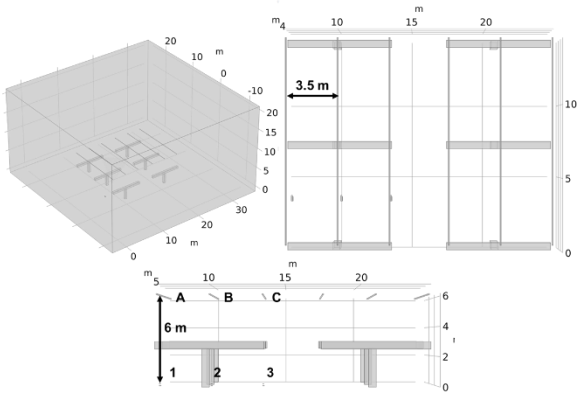

Fig. 11. 3D geometric model of the shunt reactor bay and its environment with conductors and sensors

$$C_{mat} = \begin{bmatrix} 0.0641 & 0.0311 & 0.0101 \\ 0.0325 & 0.0492 & 0.0300 \\ 0.0107 & 0.0292 & 0.0614 \end{bmatrix} pF \qquad (17)$$

Figure 12 shows the sensor voltages before the decoupling. Using the equations 13-15, the decoupling is carried out and the actual voltages on the conductors are reconstructed which are shown in figure 13. It can be seen that the voltage for all the phase voltages is near 179.6 kVp which equates to 220 kVrms × $(\sqrt{2}/\sqrt{3})$ of line voltage of the system. The measurements are very close to the actual voltages and the error in this measurement might be less than 5%.

Following the same methodology, the transients during the shunt reactor energization and de-energization are also measured using the sensor system and are shown in figures 14 and 15 respectively. It can be seen that during

the energization, due to the circuit breaker closing, it causes an EMI noise that is influencing the measurement with a very high spike in the signals. It can also be observed that there is controlled switching of circuit breakers that happens at the current zero crossings that is with regular intervals of 5 ms. From figure 15, it can be seen that there are oscillatory transients due to the sudden opening of circuit breakers, these are caused due to the capacitance in the line and the inductance of the shunt reactor. From the laboratory measurements and preliminary test results conducted at a substation, it can be seen that there is a promising solution for online monitoring of the voltages that can be used for monitoring of power system components and their insulation.

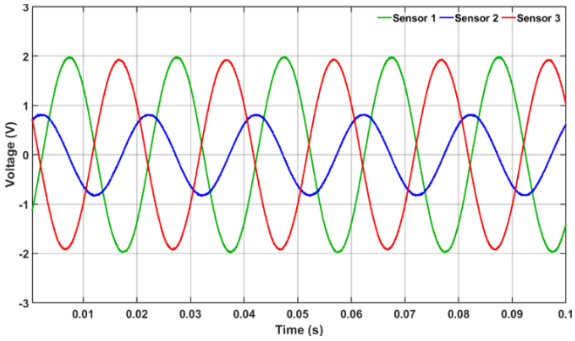

Fig. 12. Response of the sensors to three phase voltages

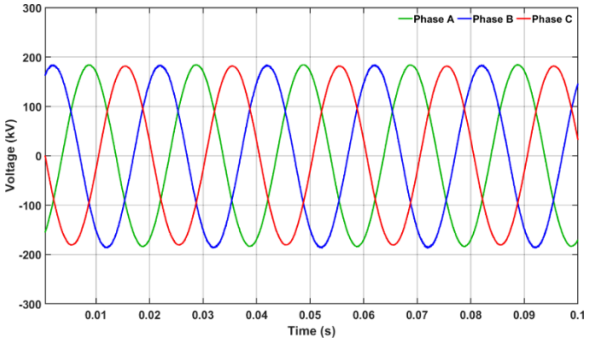

Fig. 13. Three phase voltages in the lines connecting shunt reactor after decoupling

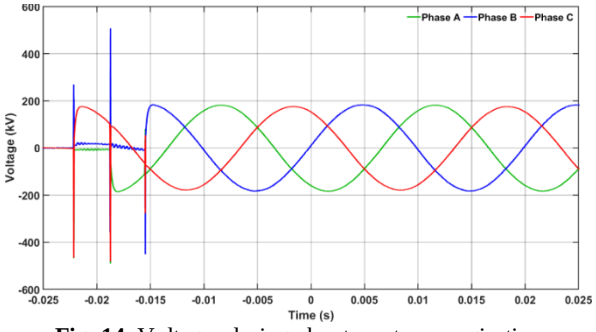

Fig. 14. Voltages during shunt reactor energization

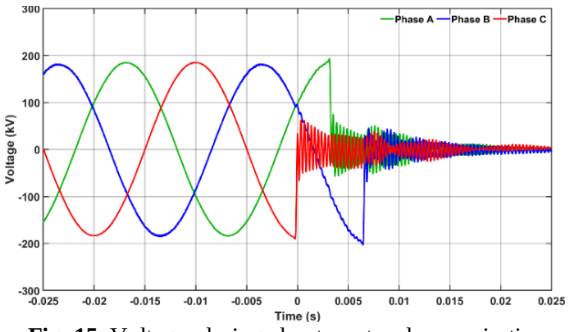

Fig. 15. Voltages during shunt reactor de-energization

5. Conclusions

From the study on the non-contact voltage measurement technique, it is confirmed that stray capacitance between the conductor and the sensor plate can be used to measure the phase conductor potentials. OP AMP based integrator gives better stability, wider frequency bandwidth capability and improve the sensitivity by increasing the signal to noise ratio which is suitable for measuring transient voltages. A laboratory test model of the three phase transmission line has been used for testing the measurement system. In a three phase voltage measurement scenario, there is cross capacitance coupling between the sensors and the conductors, so a decoupling methodology is proposed to reconstruct the actual voltages using the sensed voltages. To further test the feasibility of an online monitoring tool, measurements were carried out in a substation and shunt reactor switching transients were monitored online. Further works related to the validation of the field measurements will be carried out with power system simulation studies in future works.

6. Acknowledgement

This work was funded through SweGRIDS, by the Swedish Energy Agency, Hitachi Energy, Svenska Kraftnät and Ellevio.

7. References

[1] J.Takami, S. Okabe and E. Zaima, “Lightning Surge Overvoltages at Substations Due to Backflashover With Assumed Lightning Current Waveforms Based on Observations”, *IEEE Transactions on Power Delivery*, vol. 25, no. 4, pp. 2958-2969, 2010.

[2] CIGRE Technical Brochure 50, “Interruption of small inductive currents”, 1995.

[3] IEEE Standard 1894, “IEEE Guide for Online Monitoring and Recording Systems for Transient Overvoltages in Electric Power Systems”, 2015.

[4] J. D. Tranen and G. L. Wilson, “Electrostatically Induced Voltages and Currents on Conducting Objects under EHV Transmission Lines”, *IEEE*

Transactions on Power Apparatus and Systems, vol. 90, no. 2, pp. 768-776, 1971.

[5] W. Feser and W. Pfaff, "A Potential Free Spherical Sensor For The Measurement Of Transient Electric Fields", *IEEE Transactions on Power Apparatus and Systems*, vol. 103, no. 10, pp. 2904-2911, 1984.

[6] I. A. Metwally, "D-dot probe for fast-front high-voltage measurement", *IEEE Transactions on Instrumentation and Measurement*, vol. 59, no. 8, pp. 2211-2219, 2010.

[7] M. Schilder, "Wideband modelling of capacitive voltage sensors for open-air transmission line applications" PhD Thesis, University of Stellenbosch, 2002.

[8] D. Borkowski, A. Wetula, A. Bień, "Contactless Measurement of Substation Busbars Voltages and Waveforms Reconstruction Using Electric Field Sensors and Artificial Neural Network", *IEEE Transactions on Smart Grid*, vol. 6, no. 3, pp. 1560-1569, 2015.

[9] F. Barakou, F. Steennis, P. Wouters, "Accuracy and Reliability of Switching Transients Measurement with Open-Air Capacitive Sensors", *Energies*, vol. 12, 1405.

[10] K. -L. Chen, X. Yang, W. Xu, "Contactless Voltage Distortion Measurement Using Electric Field Sensors," *IEEE Transactions on Smart Grid*, vol. 9, no. 6, pp. 5643-5652, 2018.

[11] P. Wouters, F. Barakou, E. F. Steenis, "Application of Open-air Capacitive Sensors for Voltage Monitoring near Terminations in HV and EHV Insulated Connections", *Proceedings of Nordis Insulation Symposium*, vol. 26, pp. 70-75, 2019.

[12] P. Wouters, A. van Deursen, M. Vermeer, "Methodology and accuracy for non-invasive detection of switching transient overvoltages from compensation coils connected to power transformers", IET Science Measurement and Technology, vol. 14, pp. 173-181, 2020.

[13] Google Maps, "Torslundavägen, Fornboda, Upplands Väsby, Sweden". Accessed on 17th March 2022.